

**Probing the Adsorption of Polycyclic Aromatic Compounds onto Water
Droplets Using Molecular Dynamics Simulations**

Cuiying Jian^{†,‡}, Hongbo Zeng[†], Qingxia Liu[†], and Tian Tang^{‡,}*

[†]Department of Chemical and Material Engineering and

[‡]Department of Mechanical Engineering,

University of Alberta, Edmonton, AB, Canada

*Corresponding author; Phone: +1-780-492-5467. Fax: +1-780-492-2200.

E-mail: tian.tang@ualberta.ca

ABSTRACT: A series of molecular dynamics (MD) simulations were performed to probe the adsorption behaviors of polycyclic aromatic compounds (PACs) from *n*-heptane and toluene onto water droplets. In *n*-heptane, the simulations revealed distinct adsorbed structures of PAC molecules on the water droplets with different sizes. In the system with a small water droplet (radius 1.86 nm), the adsorbed PAC aggregate renders a straight one-dimensional (1D) structure; contrarily, in the presence of a large water droplet (radius 3.10 nm), a bent 1D structure of non-zero curvature is formed. Such size effect is a result from the delicate balance between the deformation energy required for adsorption and the available attractions between the PAC and water molecules. While the adsorbed structures are sensitive to the size of the water droplet at relatively low PAC concentration in *n*-heptane, the size effect in toluene is only prominent when the concentration of PAC molecules is sufficiently high.

1. INTRODUCTIONS

Polycyclic aromatic compounds (PACs) have drawn great interest over the past years due to their unique properties in solutions. For instance, these PAC molecules can self-assemble into aggregates of different geometries, which are of promising potential applications in the design of nano devices^{1,2} while possessing serious impact during petroleum processing.^{3,4} These PAC molecules generally contain heteroatoms (e.g. N, O) and are interfacially active, consequently they can adsorb to various interfaces such as oil/water interface. While this adsorption phenomenon is widely desired in certain areas, such as in food⁵ and cosmetics processing,^{5,6} the adsorption of certain PAC molecules, such as asphaltenes in petroleum processing, can stabilize the water-in-oil emulsions, and thus imposing deleterious effect on the water separation, facility maintenance, etc.⁷⁻⁹

Significant experimental efforts have been focused on investigating the effect of these PAC molecules on the stability of water-in-oil or oil-in-water emulsions as well as the underlying mechanisms. Earlier work of Kilpatrick and co-workers^{10,11} correlated the solvency state of asphaltene molecules to the stability of water-in-oil emulsion, and their results supported the views that the emulsions are most stable when the asphaltene molecules are at or near the point of precipitation. A series of work by Sjoblom and co-workers¹²⁻¹⁴ have investigated the effect of solvent compositions, pH, and the concentration as well as the structures of PAC molecules on the emulsion stabilities, through pulse-field gradient nuclear magnetic resonance technique, ultraviolet spectroscopy, situ Brewster angle microscopy, and atomic force microscopy. With the insights from experimental works, it was proposed^{10,13} that the formation of a rigid network/layer of PAC molecules were responsible for enhancing the emulsion stability.

Therefore, understanding the molecular arrangement of PAC compounds on the oil/water interface is crucial for stabilizing desired emulsions and destabilizing undesired emulsions.

Different adsorption forms and relative orientations of PAC molecules at the interface have been reported in literature. For instance, Sjoblom and co-workers¹²⁻¹⁴ reported continuous aggregation of PAC molecules at the xylene/water interface, and the aromatic core area of their interfacially active PAC molecules was proposed to be tilted with respect to the interface.¹² In contrast, Banerjee and co-workers¹⁵⁻¹⁸ suggested that PAC asphaltenes adsorbed on the model oil (mixtures of aliphatic base oil and toluene)/water interface were in the form of monomers with their polyaromatic cores in the plane of the interface. Such difference may be introduced by the different structures of the PAC molecules investigated in their studies. Furthermore, Mullins and co-workers^{19,20} demonstrated that the relative orientation of PAC molecules at the interface can be affected by the presence of oxygen functionality. Besides molecular structures of PAC molecules, the property of the solvent is another factor that influences the interfacial structures formed by PAC molecules. For example, from molecular dynamics (MD) simulations, while electroneutral PAC molecules were found to prefer to stay in the crude oil phase (mixtures of alkanes and aromatics) rather than migrate to the interface,²¹ evident adsorption of these electroneutral PAC models was observed at heptane/water interface with their polyaromatic cores being perpendicular to the interface.²²

While the preceding studies, and a few others,^{23,24} help to understand the structure formed at the interface, an important factor that hasn't drawn enough attention is the shape of the interfaces. For instance, in the above MD studies, flat interfaces were employed instead of

spherical ones that are usually encountered in experiments and in real applications. To bridge this gap, Liu et al.,²⁵ for the first time, simulated the adsorption of PAC molecules ($C_{47}H_{55}NS$, representing petroleum asphaltenes) onto a water droplet. The water droplet was immersed in toluene and PAC molecules were randomly distributed in the vicinity of the water droplet. It was found that the PAC asphaltene molecules formed a protective film on the interface and the stacked polyaromatic cores preferred to be perpendicular to the water surface. Despite this great effort, many important questions remain unanswered. How do the PAC molecules migrate to the interface? Will the size of the water droplets affect the adsorption of PAC molecules? If so, what is the underlying mechanism? Will such size effects depend on the concentrations of PAC molecules (note the concentration used by Liu et al., 205.3 g/L, was extremely high)? What is the role of solvent in presence of different sizes of water droplets? Answers to these questions can provide insights into understanding the adsorption behaviors of PAC molecules, which is useful for controlling emulsions and resolving relevant issues.

In this work, we performed a series of MD simulations to investigate the adsorption behaviors of the PAC molecules from *n*-heptane and toluene to water droplets of two different sizes (radii). These PAC molecules are initially dispersed in the bulk organic solvent phase, and thus can help to probe not only the final structure on the interface, but also the adsorption kinetics. More importantly, the variance in the droplet radius allows us to investigate possible structural difference at the interface caused by different drop sizes. Furthermore, employing different PAC concentrations and different solvents (toluene and *n*-heptane) provides insights on how the size effect might depend on these parameters.

2. METHODS

2.1 Systems Simulated. The PAC molecular model ($C_{46}H_{36}O_6$), shown in Figure 1, was constructed in our previous work²⁶⁻²⁹ and directly adopted here. This particular PAC molecule possesses a central aromatic core with side chains, similar to the island-type structure proposed for asphaltene molecules in literature.³⁰ It should be noted that the oxygen content in our molecule is relatively high (14 wt%) as compared to experimentally measured average oxygen weight percentage of real asphaltenes³¹ while is relatively close to that for the asphaltene fractions stabilizing oil/water emulsions.³² Furthermore, this molecular model is developed based on Violanthrone-78, therefore its study is relevant to applications in organic photovoltaic devices, near-infrared (NIR) OLEDs, and photodetectors.^{33,34} In total, six systems were designed to investigate the interfacial behaviors of PAC molecules, and their detailed information is summarized in Table 1.

Table 1. Details of the simulated systems

system	initial box size (nm ³)	initial water box size (nm ³)	no. of water molecules	no. of <i>n</i> -heptane molecules	no. of toluene molecules	no. of PAC molecules	mass conc. (g/L)	time (ns)
HEP-S	12 × 12 × 12	3 × 3 × 3	895	6070		24	15.8	100
HEP-L	14 × 14 × 14	5 × 5 × 5	4141	9447		24	9.94	100
TOL-S	12 × 12 × 12	3 × 3 × 3	895		8635	24	15.8	100
TOL-L	14 × 14 × 14	5 × 5 × 5	4141		13391	24	9.94	100
TOL-S-HC	14 × 14 × 14	3 × 3 × 3	895		13356	72	29.8	40
TOL-L-HC	14 × 14 × 14	5 × 5 × 5	4142		12683	72	29.8	40

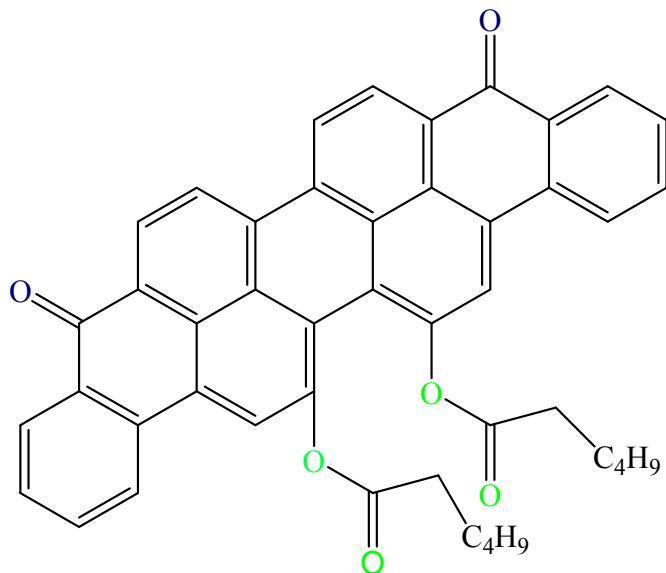


Figure 1. Molecular structure of the PAC model employed in this work. The oxygen atoms on the side chains are colored green to be distinguishable from the oxygen atoms connected only to the polyaromatic core.

The first two systems in Table 1, namely HEP-S and HEP-L, involve *n*-heptane as the solvent, each of which contains a water droplet and 24 PAC molecules. The water droplet was initially built using a cubic box filled with water molecules. Two sizes of water boxes were employed here, one of dimension $3 \times 3 \times 3 \text{ nm}^3$ (designated with -S (small) in the system names) and the other of dimension $5 \times 5 \times 5 \text{ nm}^3$ (designated with -L (large) in the system names). These two water boxes, after equilibration, form spherical water droplets of radius 1.86 and 3.10 nm, respectively, with the latter similar to that in the work of Liu et al.²⁵ The former (smaller) radius was chosen based on our previous simulations²⁸ on the same PAC molecules in pure *n*-heptane. In this study, it was found that the 24 PAC molecules simulated could self-assemble into a rod-like structure with their polyaromatic cores parallel with one another, and the length

scale of the rod-like structure is ~ 5.5 nm. Therefore the inclusion of a smaller water droplet (diameter less than 5.50 nm) helps to probe the size effect on the adsorption geometry. It should be emphasized that while the droplet sizes (\sim nm) employed here are three orders of magnitude smaller than those naturally encountered in petroleum processing ($\sim\mu\text{m}$), they are comparable to the sizes (\sim nm) of the nanoemulsions stabilized by surfactants in experiments.^{35, 36}

During constructing the initial configurations in systems HEP-S and HEP-L, the 24 PAC molecules were arranged to form a $2 \times 3 \times 4$ array surrounding the water box with their polyaromatic cores parallel with one another (see Figure 2). The rest of the simulation box was then filled with *n*-heptane molecules. Similar initial configurations were adopted in systems TOL-S and TOL-L, which had toluene as the solvent. It is worth pointing out that we kept the number of PAC molecules to be the same (24) in all these four systems. While by doing so, it resulted in different number concentrations of PAC molecules in the organic solvent phase, and different number to surface area ratios ($/\text{nm}^2$), it allows us to directly compare the number of PAC molecules adsorbed as well as the conformation formed by the PAC molecules on the water droplet surfaces of different curvatures. Particularly, as mentioned above, it was shown in our previous work²⁸ that 24 PAC molecules could aggregate into well-defined 1D structure in *n*-heptane in absence of water droplets. Therefore it is of great interest to adopt the same amount of PAC molecules and investigate whether and how water droplets of different radii might alter their self-assembled structures through adsorption.

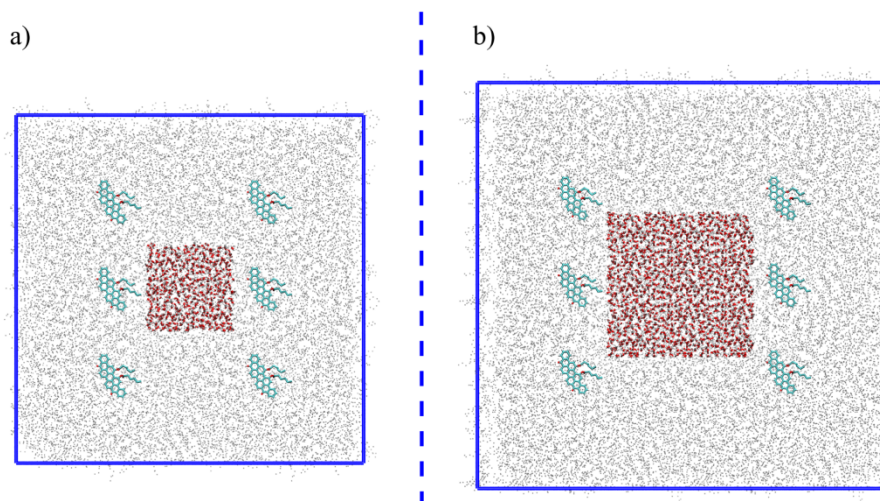


Figure 2. Initial configurations (side views) for systems: a) HEP-S and TOL-S and b) HEP-L and TOL-L. PAC molecules are mainly colored cyan and water molecules colored red; gray points represent organic solvents.

In addition to the above four simulations, we performed two additional simulations with toluene being the solvent, namely TOL-S-HC (“HC” representing “high concentration”) and TOL-L-HC, in which 72 PAC molecules were initially packed into an ordered array. These two systems differ by the size of the water droplet. The reason for performing these two simulations in toluene is that, due to the good solubility of the PAC molecules in toluene,²⁷ sufficiently high concentrations may be needed to observed evident adsorption and size effect.

2.2 Simulation Details. The molecular topologies for PAC, *n*-heptane and toluene molecules were validated in our previous work,²⁶⁻²⁹ and directly adopted here; a simple-point-charge (SPC) model³⁷ was used for water molecules, which has been extensively tested in literature for interfacial studies.^{23,38,39} Particularly, the PAC topology was first generated by supplying the coordinates of the molecule to the GlycoBioChem PRODRG2 server.⁴⁰ The default topology

obtained from PRODRG was then corrected using non-bonded parameters from GROMOS96 53A6 force field.⁴¹ Such correction is needed to remove the artifacts existing in the default topology,⁴² and the so-generated topology has been validated by comparing the mean separation between $\pi - \pi$ stacked polyaromatic cores from simulations with that from experimental studies.^{26,43}

All simulations were performed using the MD package GROMACS⁴⁴⁻⁴⁷ with periodic boundary conditions applied. For each system, static structure optimization was first performed to ensure that the maximum force is less than 1000.0 kJ/(mol·nm), followed by dynamics simulation in NPT ensemble (40 ns for systems TOL-S-HC and TOL-L-HC, and 100 ns for the other systems). For all full dynamics simulations, the pressure was kept at 1 bar by Parrinello-Rahman barostat,⁴⁸ temperature was kept at 300 K by velocity rescaling thermostat,⁴⁹ which is based on correctly producing the probability distribution of kinetic energy under constant temperature; the integration time step was 2 fs; intra-molecular bonds for water molecules were constrained by the SETTLE algorithm⁵⁰ and all the other molecules by the LINCS algorithm;⁵¹ full electrostatics was treated by particle-mesh Ewald method;⁵² and van der Waals interactions were evaluated by a cutoff approach with cutoff distances 1.4 nm. Appropriate postprocessing programs available in GROMACS were used for trajectory analysis and VMD⁵³ for visualization.

3. RESULTS AND DISCUSSION

3.1 Adsorption Characteristics and Mechanisms. To identify whether PAC molecules migrated to the water droplet or not in the two solvents, we first monitored the size (n_1) of the largest cluster formed by water and PAC molecules as well as the number of water molecules

(n_2) involved in this cluster. Here, size of the cluster is the number of associated molecules (including both PAC and water molecules), which are determined using a single linkage algorithm⁵⁴ with cutoff distance 0.5 nm. Correspondingly, the largest cluster is defined as the cluster with the largest number (n_1) of associated molecules. Then the number of PAC molecules connected to the water droplet in the largest cluster is given by $n = n_1 - n_2$, and is plotted versus simulation time in Figure 3a.

The first observation made from Figure 3a is that all the curves exhibit quite dynamic behaviors with fluctuations in the curve along the simulation time. The fluctuation can have a magnitude of one at sometime, but a significant fraction of the fluctuations also involve more than one PAC molecules. This indicates that the PAC molecules can attach to and detach from the water droplet as individuals or in an aggregated form. Furthermore, by comparing the four curves in Figure 3a, it can be seen that, dramatic differences exist between the systems with *n*-heptane as solvents and those with toluene as solvents. For systems HEP-S and HEP-L, the migration of PAC molecules onto the water droplet continues for a period of time, evidenced by the growing number in Figure 3a; these numbers reach 24 in the late stage of the simulation, corresponding to all of the 24 PAC molecules connected to the water droplet. On the other hand, for system TOL-L, on average, only ~ 6 molecules are connected to the water droplet; for system TOL-S, from ~ 35 ns to 85 ns, half of the simulation time, not a single PAC molecule is in connection with the water droplet. That is, in *n*-heptane, PAC molecules migrate to the interface and their adsorption tends to be irreversible,¹⁷ while in toluene, they are more prone to being solvated in the bulk toluene phase, and completely detachment, i.e. reversible adsorption, is observed. These observations confirm that these PAC molecules are more soluble in toluene than

in *n*-heptane, which is consistent with the solubility definitions of asphaltenes that these PAC molecules represent.^{55,56}

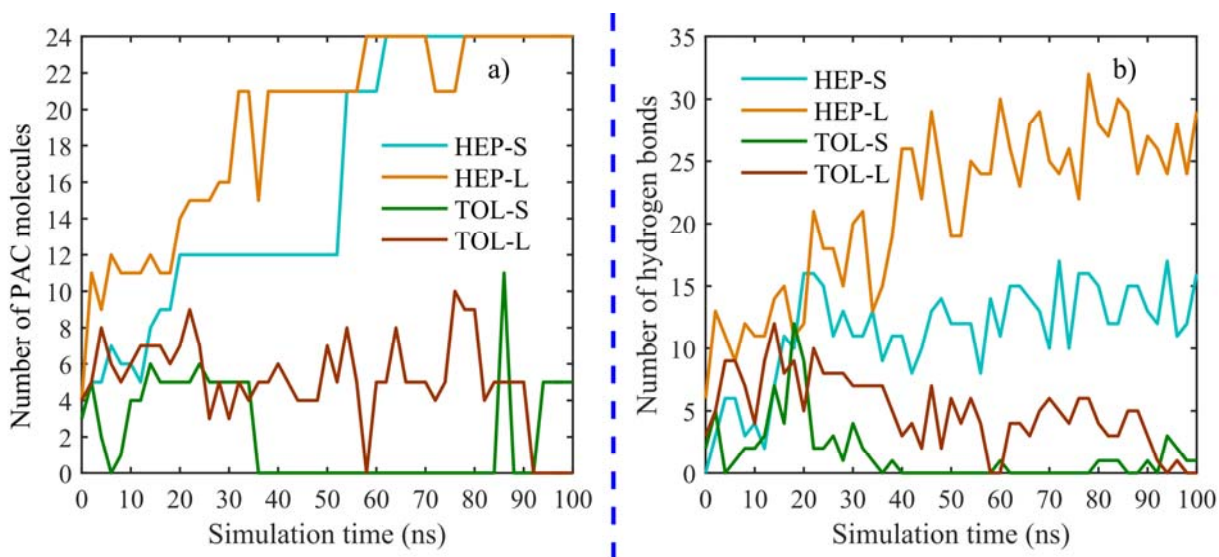


Figure 3. a) Number of PAC molecules connected to the water droplet in the largest cluster and b) number of hydrogen bonds formed between all PAC molecules and water droplets in the simulated systems, both plotted against simulation time.

To probe the underlying mechanisms on the distinct kinetics observed above, we calculated the number of hydrogen bonds, formed between all the PAC molecules and water, for the four systems (Figure 3b). As it can be seen, the curves for PAC molecules in *n*-heptane exhibit a substantial increase at the initial stage of the simulation, followed by stabilization, corresponding to the adsorption of PAC molecules onto the water droplet. For PAC molecules in toluene, while an initial increase is still observed, in the late stage of the simulation (from ~40 ns to 100 ns), the number decreases to 0 and ~5, respectively, in systems TOL-S and TOL-L. Clearly, toluene depressed the formation of hydrogen bonds between PAC and water molecules, indicating that the PAC-water interaction in toluene is much weaker than that in *n*-heptane. This

can be attributed to the strong attractions between toluene and polyaromatic cores demonstrated in our previous work,²⁷ which prevent PAC molecules from effectively interacting with the water droplet. It is of great importance to point out that as PAC molecules are highly polarizable,⁵⁷ in addition to hydrogen bonds, other types of electrostatic forces, such as induced dipole-induced dipole interactions, can also play important roles for the adsorption of PAC molecules to the oil/water interfaces.

As shown above, while solvents demonstrate profound effects on the adsorption of PAC molecules, it seems that sizes of the water droplets exhibit insignificant effect on the adsorption kinetics of PAC molecules. However, detailed examination of Figure 3 revealed that while all 24 PAC molecules are connected to the water droplet in both systems HEP-S and HEP-L, different numbers of hydrogen bonds are formed between PAC and water molecules, especially in the late stage of the simulation time (on average < 15 for HEP-S while > 25 for HEP-L). This suggests that the PAC-water interaction in the system containing a small water droplet is smaller than that in the system having a larger water droplet, and distinct adsorbed structures may have been formed by PAC molecules on the droplets of different curvatures. Below, we will take a detailed look at these structures.

3.2. Size Effect on the Adsorbed Structures in *n*-Heptane. Figure 4 shows the final configurations formed in systems HEP-S and HEP-L. As can be seen, in each system the PAC molecules adsorbed to the water droplet form a single aggregate with the polyaromatic cores of adjacent molecules parallel with one another. This suggests that during the migration and attachment to the water droplet, the PAC molecules are able to reorganize themselves into

parallel stacking, driven by the interactions between polyaromatic cores.²⁶⁻²⁹ To further probe which part (core or side chain) of the PAC molecules are contacting with water, in Figure 5, we plotted the radial distribution function (RDF) for the oxygen atoms in PAC molecules with respect to the oxygen atoms of the water molecules. In Figure 5, each plot contains two curves: one for RDF between the oxygen atoms on the polyaromatic cores (colored dark blue in Figure 1) and the oxygen atoms of water, whereas the other for RDF between the oxygen atoms on the side chains (colored green in Figure 1) and the oxygen atoms of water. It can be seen that, for each system, the peak of the RDF curve for the oxygen on the cores is much higher than that for the oxygen atoms on the side chains, indicating that the polyaromatic cores are directly contacting with water, while the side chains are staying away. To simultaneously promote the $\pi - \pi$ stacking between the polyaromatic cores and the attraction between oxygen atoms on the cores with water, the aggregates of the PAC molecules tend to have an orientation that is perpendicular to the water surface where they contact. This observation, made for both HEP-S and HEP-L, shares great similarity to the experimental study of Andrews et al.,¹⁹ where polyaromatic cores of Violanthrone-78 are reported to be perpendicular to the solvent/water interface.

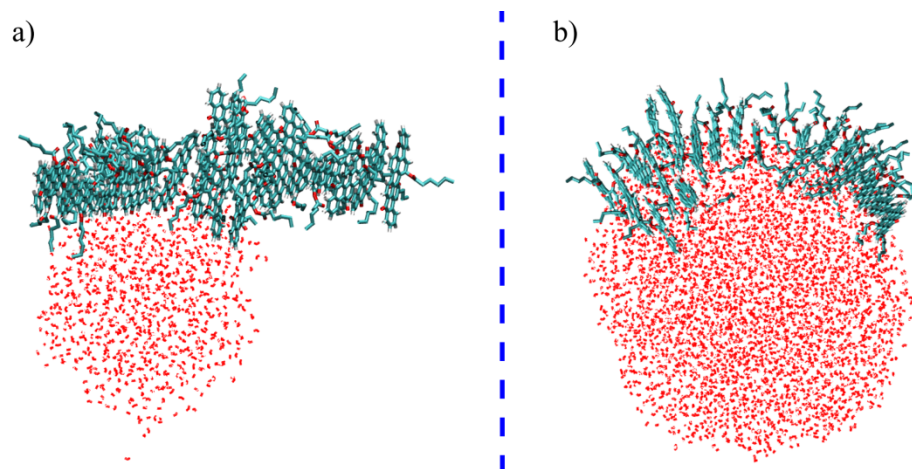


Figure 4. Final configurations formed in systems a) HEP-S and b) HEP-L: water molecules are in red and PAC molecules in cyan; *n*-heptane molecules are removed for clarity.

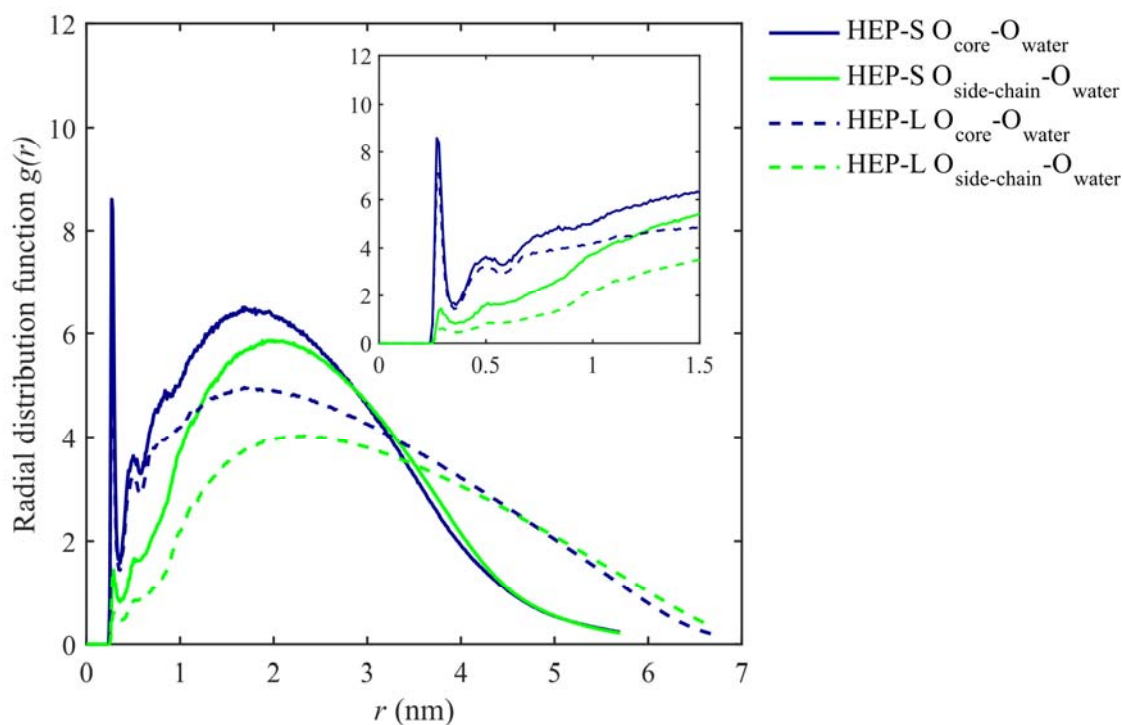


Figure 5. RDFs of oxygen atoms in PAC molecules around oxygen atoms in water. The inset shows the enlarged RDFs at short distances.

Despite the above similarities, distinct differences can be found in the adsorbed structures (Figure 4) formed in the two systems. In system HEP-S, only 50% of the PAC molecules are in direct contact with the water droplet, while the rest are embedded in the bulk *n*-heptanes without direct connection to water. In contrast, for system HEP-L, all the 24 PAC molecules are directly contacting water. The different adsorption can be further verified by examining the distribution of polyaromatic cores around the water droplet. For this purpose, we plotted the cumulative numbers of polyaromatic cores with respect to the water droplet surface in Figure 6. Here, each polyaromatic core was represented using a central atom on the core plane (for the choice of this central atom, see Supporting Information, section S1), and the cyan and orange curves indicate the total number of cores within a given distance to their nearest water molecules, respectively for systems HEP-S and HEP-L. Therefore, the so-defined cumulative number essentially describes the amount of PAC molecules located within a given distance from the surface of the water droplet. As it can be seen, within the same separation distance r_1 , more PAC molecules can be found in system HEP-L compared to those in system HEP-S. For instance, at $r_1 = \sim 1.2$ nm, the cumulative number for system HEP-L is 24, indicating that all the 24 polyaromatic cores are located within ~ 1.2 nm from the water surface. In contrast, at the same distance, for system HEP-S, only ~ 13 cores are found, and the rest ~ 11 molecules are at 1.2-3.5 nm from the water surface. That is, in system HEP-S, nearly 50% of the PAC molecules have no close contact with the water droplet and are embedded in the bulk *n*-heptane phase. These data are consistent with our visual observation in Figure 4.

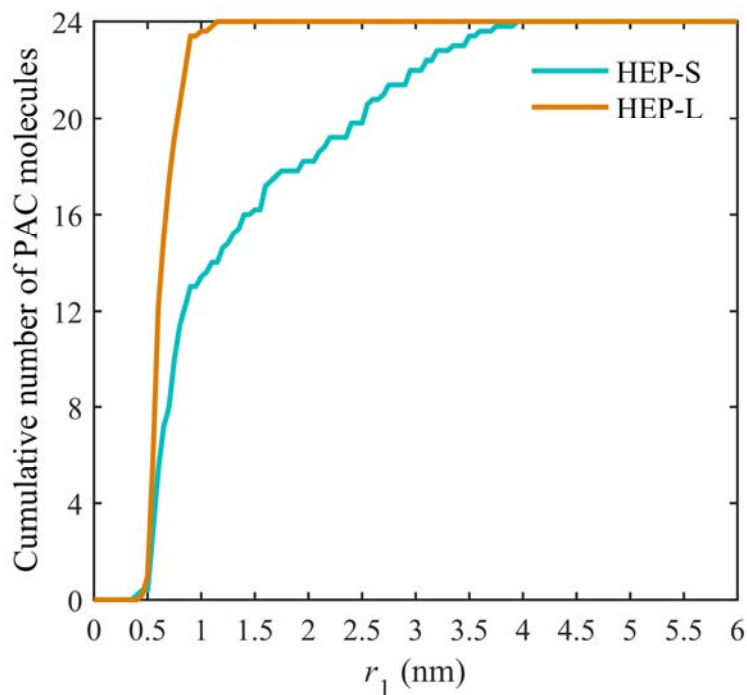


Figure 6. Cumulative number of polyaromatic cores as a function of the distance r_1 from the water droplet surface.

The different relative positions of PAC molecules, with respect to the water droplets, can have profound effects on the geometries of the structures formed by PAC molecules. In system HEP-S (Figure 4a), the aggregate is more or less straight, rendering a one-dimensional (1D) rod-like structure with a nearly zero curvature, whereas in system HEP-L (Figure 4b), the aggregate is confined to the water droplet, and thus having a non-zero curvature. To quantitatively compare the geometries of the PAC aggregates, we calculated the cosine of angle σ ($\cos \sigma$) between any two core planes and the distance d between the corresponding centers of geometry (COGs) (for details on the calculation of $\cos \sigma$ and COG distances, see Supporting Information, section S2). Figure 7 shows $\cos \sigma$ versus the COG distance d for the two systems in *n*-heptane. In each system, the aggregate consists of all 24 molecules; hence there are in total $C_{24}^2 = (24 \times 23)/2 =$

276 pairs of cores and 276 data points. For system HEP-S, most of the data are distributed around $\cos \sigma = 0.92$, confirming that polyaromatic cores are parallel with one another (Figure 4a) even at very large separation distances. On the contrary, the data points are distributed over the range of $\cos \sigma = 0.2 - 1$ in system HEP-L, demonstrating that as the PAC molecules confine themselves to the water droplet (Figure 4b), the parallel stacking between non-neighboring cores is disrupted. The different range of parallel stacking can then result in different geometries of the PAC aggregates. Adopting the methodology proposed in our recent work,⁵⁸ for a “perfectly” straight 1D structure, its two gyradius ratios will be approximately equal and $\gg 1$. Here, for aggregates in systems HEP-S and HEP-L, the corresponding gyradius ratios are, respectively, {2.52, 2.63} and {1.8, 1.95}. Clearly, the gyradius ratios in the presence of a relatively smaller water droplet are much larger than those in the presence of a relatively larger water droplet, quantitatively confirming that a straight rod-like structure is formed in system HEP-S while the structure formed in system HEP-L is bent, due to the confinement.

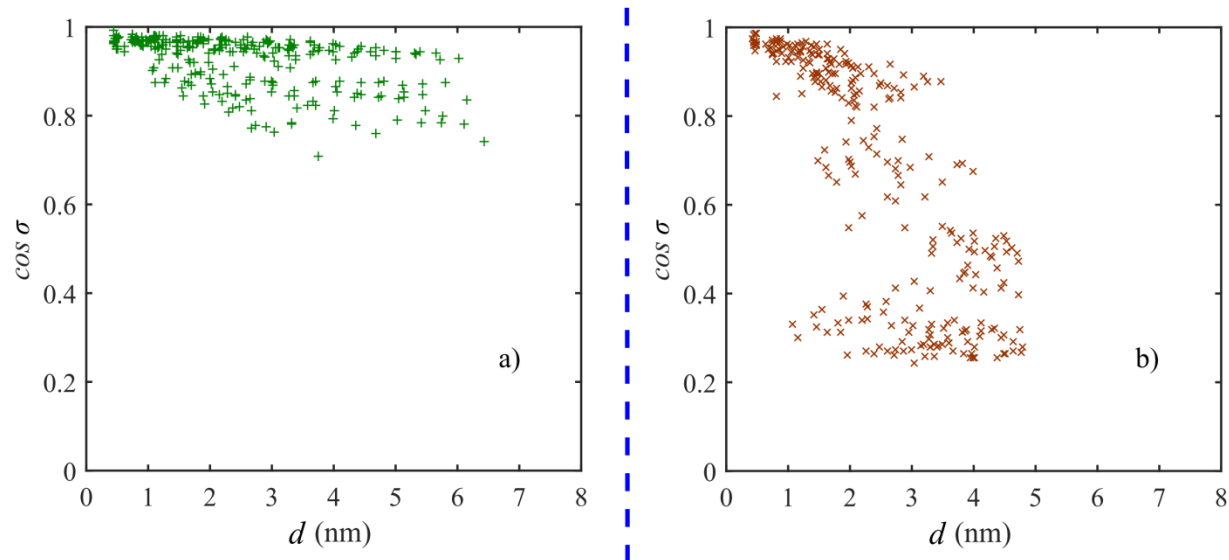


Figure 7. $\cos \sigma$ versus the COG distance d for the aggregates formed in systems a) HEP-S and b) HEP-L.

To bend a structure, sufficient amount of energy is needed. In our current study, as discussed in section 3.1, electrostatic attractions exist between PAC and water molecules. These attractions can potentially have two roles: 1) to promote the migration of PAC molecules from organic solvents onto the water droplet and anchor the aggregates, and 2) to bend the aggregates and confine these PAC molecules to the water droplet. Because *n*-heptane is a “poor” solvent for PAC molecules, the PAC molecules experience little difficulty in migrating from *n*-heptane to the interface. As a result, in both HEP-S and HEP-L all 24 PAC molecules are clustered in an aggregate anchored to the interface. In the scenario where the diameter of the water droplets is small compared to the length scales of the aggregate, a great amount of elastic bending energy is required to confine the aggregate to the droplet, and this energy may exceed what can be provided by the PAC-water interactions. Hence, the aggregate remains straight and some of the PAC molecules are embedded in the bulk organic solvent (Figure 4a). In this case, the PAC-

water interactions only serve to promote the migration and anchor the aggregates. If we consider the opposite extreme where the diameter of the water droplet is much larger than the length scales of the aggregates, the energy needed to bend the aggregates is negligible because of the small curvature, and the anchored aggregate is expected to, again, render a straight rod-like structure that conforms to the nearly flat interface. For water droplets of intermediate sizes, the interactions between the PAC and water molecules are sufficient to not only anchor the PAC molecules, but also bend the aggregates and confine the PAC molecules onto the water droplet. Therefore a bent rod of a non-zero curvature can be observed (Figure 4b).

3.3. Size Effect at High Concentration in Toluene. As discussed in section 3.1, PAC molecules prefer to stay in the bulk toluene phase in systems TOL-S and TOL-L regardless of the water droplet size, although the probability of the PAC molecules in contact with water is slightly higher in system TOL-L. The slightly higher probability can be attributed to the larger surface area of the larger droplet, which increases the contact probability between the PAC and water molecules. Intuitively the contact probability can also be increased by introducing more PAC molecules in the system; therefore it is of interest to examine the adsorption behavior of PAC molecules under a higher concentration. To do so, we increased the number of PAC molecules from 24 to 72, resulting in two additional simulations TOL-S-HC and TOL-L-HC. These two systems are of the same box dimensions and differ in the size of the water droplets as well as the number of toluene molecules.

We first monitored the adsorption kinetics in these two systems, using the same procedure described in section 3.1; this is shown in Figure 8. Clearly, for system TOL-S-HC,

while the concentration was increased compared to system TOL-S, no adsorption was observed for most of the simulation time; on the other hand, for system TOL-L-HC, in comparison with system TOL-L, with the increased concentration the number of PAC molecules connected to the water droplet was on average ≥ 18 after the simulation started. This is consistent with the final configurations shown in Figure 9, where PAC molecules are mainly distributed in the toluene phase in system TOL-S-HC (Figure 9a), while in system TOL-L-HC, some PAC molecules are adsorbed onto the water droplet (Figure 9b, highlighted in the purple ellipse).

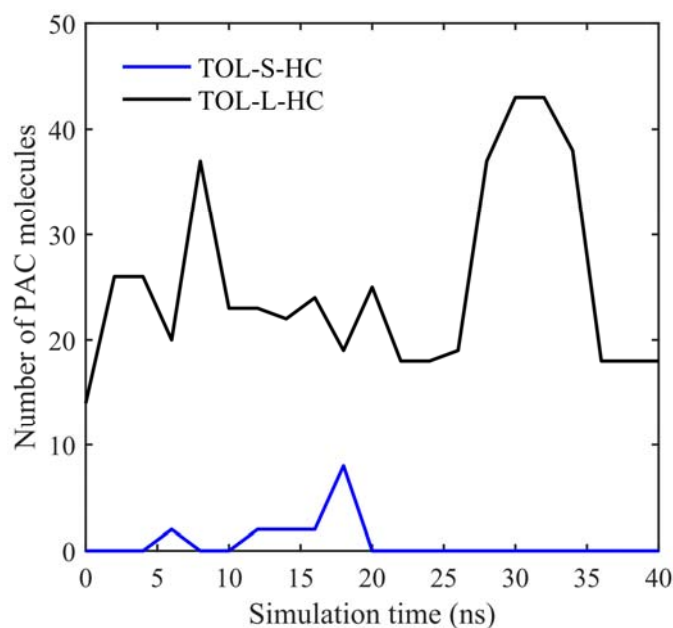


Figure 8. Number of PAC molecules connected to the water droplet versus simulation time.

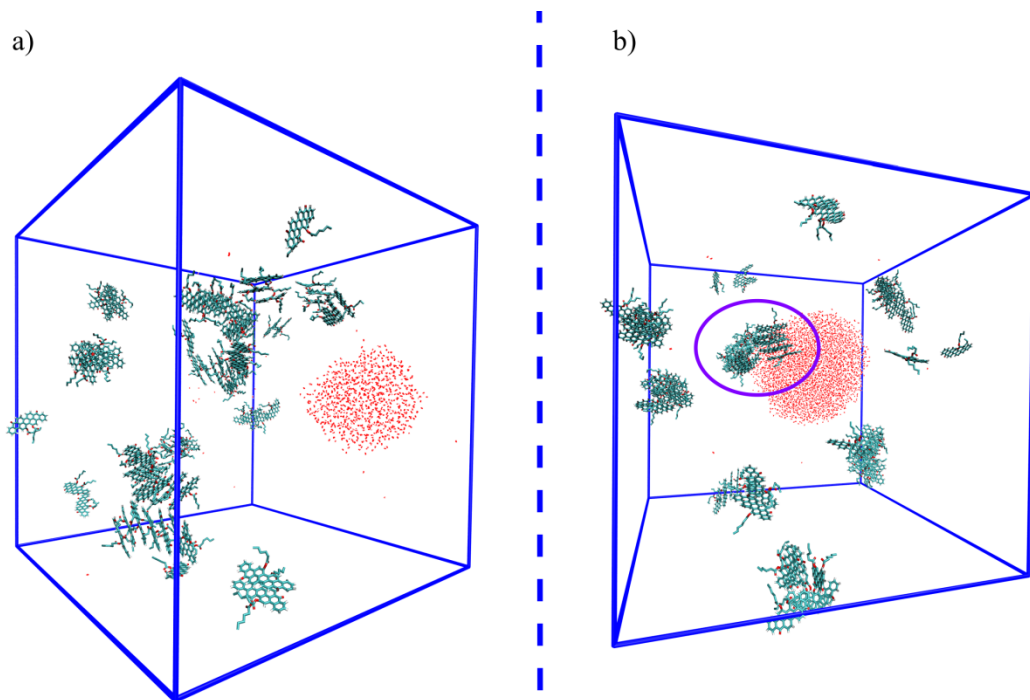


Figure 9. Final configurations formed in systems a) TOL-S-HC and b) TOL-L-HC. Blue lines represent simulation boxes, and water molecules are in red with PAC molecules in cyan. Toluene molecules are removed for clarity.

The above observations indicate that, at higher concentrations, sizes of the water droplets can also have profound effects on the adsorption of PAC molecules in toluene. Unlike in *n*-heptane, great attractions exist between solute PAC cores and toluene molecules,²⁷ which not only disfavors the aggregation of PAC molecules²⁷ but also hinders their migration to the water/toluene interface²⁰. Hence significant effort is required for the PAC molecules to overcome the solute (PAC)-solvent (toluene) attraction and migrate to the interface, as well as for the water droplet to anchor these PAC molecules. At lower PAC concentrations, since the PAC molecules are sparsely dispersed in toluene, the interactions between PAC molecules as well as those between PAC molecules and the water droplet are limited, and the PAC-toluene attraction is

dominant; this leads to the insignificant adsorption regardless of the size of the water droplet (Figure 3a). However, increasing the concentration results in enhanced PAC molecular aggregation as well as a larger contact probability between PAC and water molecules. The enhanced aggregation can help to reduce the exposure of the solutes to the toluene, and meanwhile the increased contact probability can directly favor the adsorption of PAC molecules. Hence with the presence of a large water droplet, the PAC-water attractions may be able to exceed the PAC-toluene attraction, enabling the migration and further anchoring of the PAC aggregates coming into contact with the droplet (Figures 8b and 9b). On the other hand, in the case of a small water droplet, while the contact probability can be potentially higher than the system with low PAC concentration, limited by the number of water molecules, the attraction between PAC and water molecules may still be insufficient to drive the migration or anchor the PAC molecules (Figures 8 and 9a).

It is important to point out here that while initially 13 PAC molecules were in connection with the water droplet in system TOL-L-HC (Figure 8, time = 0 s), the final adsorption of PAC molecules should not be attributed to the choice of initial configurations (for demonstration of deviating from the initial configuration using correlation function, see Supporting Information, section S3). Rather from the preceding analysis, it should be attributed to the higher contact probability and stronger PAC-water attractions present in the system. As another example, in systems TOL-S and TOL-L, initially adsorbed PAC molecules (3 to 4 molecules in Figure 3a) could be completely detached from the water droplet as the simulations started.

Finally, as mentioned in section 2.1, different concentrations were employed when the size of the water droplet was changed. Table 2 summarizes the number ratio (c_1) as well as the number to surface area ratio (c_2 , /nm²) of PAC molecules for each system. c_1 is defined as the ratio between the number of PAC molecules and the number of organic solvent molecules, and c_2 is the ratio of the number of PAC molecules over the surface area of the water droplet. As can be seen, c_1 and c_2 in systems containing a larger water droplet are always smaller than their counterparts with a smaller water droplet, except c_1 in system TOL-L-HC (almost the same as c_1 in system TOL-S-HC). Nevertheless, complete confinement (better adsorption) of PAC molecules was observed in system HEP-L compared to that in system HEP-S, and more evident adsorption of PAC molecules was found in systems TOL-L and TOL-L-HC in comparison to systems TOL-S and TOL-S-HC. Therefore if we apply the c_1 and c_2 values in the systems containing a small water droplet to the systems of a large water droplet, we should still expect bent rods of PAC molecules conforming to the interface in system HEP-L, and much more evident adsorptions in systems TOL-L and TOL-L-HC.

Table 2. The number ratio (c_1) and the number to surface area ratio (c_2 , /nm²) of PAC molecules for all systems studied.

System	Number ratio of PAC (c_1)	Number to surface area ratio (c_2 , /nm ²)
HEP-S	0.0040	0.5520
HEP-L	0.0025	0.1987
TOL-S	0.0028	0.5520
TOL-L	0.0018	0.1987
TOL-S-HC	0.0054	1.6561
TOL-L-HC	0.0057	0.5962

3.4. Implications. As discussed in section 3.2, 1D rod-like aggregates are formed in systems HEP-S and HEP-L. This type of structure is of great potential applications in the design of optical and electronic devices.^{1,2} In our previous work,^{28,29} we have discussed the solvent and solute conditions to achieve such types of structures. Here, the formation of 1D structure in the presence of water droplets suggests that the inclusion of a polar phase, such as water droplets, can help to further control the geometry of the structure. For instance, the sizes of the water droplets have significant effects on the curvature of the adsorbed structures. Therefore by selecting suitable water droplets, 1D structures with prescribed curvature can be obtained.

Furthermore, while the droplet sizes studied in our work are limited by current available computational capacity, as our PAC molecules share great similarities to industrial asphaltene compounds, the results discussed here also provide us with insights into the water-in-oil emulsions usually encountered in petroleum processing. Consistent with the work of Liu et al.,²⁵ the core areas of PAC molecules form close contact with the water molecules, and are in an aggregated state (Figure 4). This observation confirms previous experimental postulations^{10,13} that PAC molecules form a thin film on the surface of the water droplet during petroleum processing, and thus preventing water droplets from coalescence. However it should be noted that the specific adsorption form and orientation observed here and in existing literature²⁰⁻²⁵ can strongly depend on the molecular structure as well as the concentration of the PAC compounds. Specifically, in our current work, the PAC molecules have two relatively short linear side chains and both of them are localized at the same bay region of the core. Therefore these side chains have insignificant steric hindrance to the stacking of the polyaromatic cores. Under a high concentration (>9 g/L, 1.31 wt% in organic phase of all simulations), the stacking is evident,

leading to the observation that the adsorbed PAC molecules are in an aggregated state with their polyaromatic cores parallel with one another. On the other hand, in some literature, such as in the work of Banerjee and co-workers,¹⁵⁻¹⁸ experimental measurements suggested only monomer adsorption of PAC asphaltenes onto model oil/water interface. Compared with our work here, the difference could be caused by the following factors: 1) the concentration of asphaltenes was low (≤ 500 ppm, 0.05 wt%), and 2) the asphaltene molecules were proposed to have branched side chains distributed peripherally around the polyaromatic core area, which may introduce prominent steric hindrance to the stacking and further prevent the aggregation on the interface. In addition, the perpendicular orientation of PAC molecules observed here can be partly attributed to the oxygen functional groups, such as ketone and ester, present in the chemical structures. For PAC molecules without oxygen moieties, their polyaromatic core may prefer parallel to the interface, as reported by Banerjee and co-workers.¹⁵⁻¹⁸ Indeed, it has been suggested by Mullins and co-workers^{19,20} that the presence of oxygen moiety can alter the preferred orientations of PAC molecules from being parallel to being perpendicular. As our molecular model, as well as the ones used in other literature²⁰⁻²⁵, only mimics certain features of the complex asphaltene molecular structures, care should be taken in inferring the interfacial structures in general.

More interestingly, in our current work, although the bulk concentration of PAC molecules is very high (>9 g/L, 1.31 wt% (0.015 M) in organic phase of all simulations), the amount of PAC molecules is still not enough to fully cover the water droplet, even in *n*-heptane as shown in Figure 4. While Liu et al.²⁵ reported the formation of protective film using MD simulations, the concentrations employed in their work is extremely high (205.3 g/L, 0.66 M). Contrarily, the water-in-oil emulsions are reported to be stabilized by PAC molecules at very low

concentrations in experiments.^{13,59} For instance, in the work of Nenningsland et al.,¹³ the emulsions were completely stable for all concentrations of their model PAC molecules above 0.08 mM in xylene. These seemingly contradictory findings should be attributed to the difference between “local concentration” and “bulk concentration”. That is, when the emulsions are being stabilized in experiments, i.e., when a thin film of PAC molecule are being formed around the water droplet, the “local concentration” of PAC molecules accumulated in the vicinity of the interface can be much higher than the “bulk concentration”.⁶⁰ Therefore, these discussions provided justification for MD simulations to adopt high concentrations in order to study adsorption behaviors of interfacial-active molecules. Furthermore, when cross comparison is needed between experiments and simulations, one should always take care and avoid using bulk concentration as the only parameter.

Finally, as our droplet sizes employed here are directly comparable to the nanoemulsions stabilized by surfactants in experiments³⁶, the discussion presented here can provide valuable information for preparing desired nanoemulsions. For instance, it can help with predicting the adsorbed structures of aromatic surfactant onto the droplets.

4. CONCLUSIONS

In this work, we employed all-atom MD simulations to investigate the adsorption behaviors of PAC molecules onto water droplets in *n*-heptane and toluene. With *n*-heptane as the solvent, while regardless of the water droplet size, all PAC molecules can easily migrate to the interface and the adsorbed PAC molecular aggregates renders 1D rod-like structure, we found that the water droplet size can have profound effects on the curvatures of the PAC aggregates. That is, in

the system involving a small water droplet, the 1D structure is more or less straight with 50% of PAC molecules embedded in the bulk *n*-heptane phase; contrarily, in the system having a large droplet, the 1D structure is confined to the droplet surface and thus having a non-zero curvature. The formation of these different adsorbed structures seems to be determined by the deformation energy required as well as the available attractions present between the PAC and water molecules. Compared to that in *n*-heptane, the adsorption of PAC molecules in toluene requires significant attractions from water molecules to overcome the PAC-toluene attraction. Therefore evident adsorption of PAC molecules in toluene was only observed at a sufficiently high concentration with the presence of a large water droplet. The results reported here provide fundamental insights into how the adsorption of the PAC molecules can be modulated by the size of the water droplets and property of the organic solvents.

ACKNOWLEDGEMENTS

We acknowledge the computing resources and technical support from Western Canada Research Grid (WestGrid). Financial support from the Natural Science and Engineering Research Council (NSERC) of Canada and Canadian Centre for Clean Coal/Carbon and Mineral Processing Technologies (C⁵MPT) is gratefully acknowledged.

SUPPORTING INFORMATION

Representation of the polyaromatic core using a central atom, details on the calculation of $\cos \sigma$ and COG distances, and time correlation function for the minimum distances between PAC molecules and water droplet.

REFERENCES

- (1) Zang, L.; Che, Y.; Moore, J. S. One-Dimensional Self-Assembly of Planar π -Conjugated Molecules: Adaptable Building Blocks for Organic Nanodevices. *Acc. Chem. Res.* **2008**, *41*, 1596-1608.
- (2) Kim, F. S.; Ren, G.; Jenekhe, S. A. One-Dimensional Nanostructures of π -Conjugated Molecular Systems: Assembly, Properties, and Applications from Photovoltaics, Sensors, and Nanophotonics to Nanoelectronics†. *Chemistry of Materials* **2010**, *23*, 682-732.
- (3) Groenzin, H.; Mullins, O. C. Asphaltene Molecular Size and Structure. *The Journal of Physical Chemistry A* **1999**, *103*, 11237-11245.
- (4) Speight, J. Petroleum Asphaltenes-Part 1: Asphaltenes, Resins and the Structure of Petroleum. *Oil & gas science and technology* **2004**, *59*, 467-477.
- (5) Ghosh, S.; Rousseau, D. Fat Crystals and Water-in-Oil Emulsion Stability. *Current Opinion in Colloid & Interface Science* **2011**, *16*, 421-431.
- (6) Yoneyama, T.; Yamaguchi, M.; Tobe, S.; Nanba, T.; Ishiwatari, M.; Toyoda, H.; Nakamura, S.; Kumano, Y.; Takata, S.; Ito, H. *Water-in-oil emulsion type cosmetics* **1991**, .
- (7) Mouraille, O.; Skodvin, T.; Sjöblom, J.; Peytavy, J. Stability of Water-in-Crude Oil Emulsions: Role Played by the State of Solvation of Asphaltenes and by Waxes. *J. Dispersion Sci. Technol.* **1998**, *19*, 339-367.
- (8) Spiecker, P. M.; Gawrys, K. L.; Trail, C. B.; Kilpatrick, P. K. Effects of Petroleum Resins on Asphaltene Aggregation and Water-in-Oil Emulsion Formation. *Colloids Surf. Physicochem. Eng. Aspects* **2003**, *220*, 9-27.
- (9) Kilpatrick, P. K. Water-in-Crude Oil Emulsion Stabilization: Review and Unanswered Questions. *Energy Fuels* **2012**, *26*, 4017-4026.
- (10) McLean, J. D.; Kilpatrick, P. K. Effects of Asphaltene Solvency on Stability of Water-in-Crude-Oil Emulsions. *J. Colloid Interface Sci.* **1997**, *189*, 242-253.
- (11) McLean, J. D.; Kilpatrick, P. K. Effects of Asphaltene Aggregation in Model heptane–toluene Mixtures on Stability of Water-in-Oil Emulsions. *J. Colloid Interface Sci.* **1997**, *196*, 23-34.
- (12) Nordgård, E. L.; Sørland, G.; Sjöblom, J. Behavior of Asphaltene Model Compounds at W/O Interfaces. *Langmuir* **2009**, *26*, 2352-2360.
- (13) Nenningsland, A. L.; Gao, B.; Simon, S.; Sjöblom, J. Comparative Study of Stabilizing Agents for Water-in-Oil Emulsions. *Energy Fuels* **2011**, *25*, 5746-5754.

- (14) Bi, J.; Yang, F.; Harbottle, D.; Pensini, E.; Tchoukov, P.; Simon, S.; Sjöblom, J.; Dabros, T.; Czarnecki, J.; Liu, Q. Interfacial Layer Properties of a Polyaromatic Compound and its Role in Stabilizing Water-in-Oil Emulsions. *Langmuir* **2015**, *31*, 10382-10391.
- (15) Rane, J. P.; Harbottle, D.; Pauchard, V.; Couzis, A.; Banerjee, S. Adsorption Kinetics of Asphaltenes at the oil–water Interface and Nanoaggregation in the Bulk. *Langmuir* **2012**, *28*, 9986-9995.
- (16) Rane, J. P.; Pauchard, V.; Couzis, A.; Banerjee, S. Interfacial Rheology of Asphaltenes at oil–water Interfaces and Interpretation of the Equation of State. *Langmuir* **2013**, *29*, 4750-4759.
- (17) Pauchard, V.; Rane, J. P.; Zarkar, S.; Couzis, A.; Banerjee, S. Long-Term Adsorption Kinetics of Asphaltenes at the Oil–Water Interface: A Random Sequential Adsorption Perspective. *Langmuir* **2014**, *30*, 8381-8390.
- (18) Rane, J. P.; Zarkar, S.; Pauchard, V.; Mullins, O. C.; Christie, D.; Andrews, A. B.; Pomerantz, A. E.; Banerjee, S. Applicability of the Langmuir Equation of State for Asphaltene Adsorption at the Oil–Water Interface: Coal-Derived, Petroleum, and Synthetic Asphaltenes. *Energy Fuels* **2015**, *29*, 3584-3590.
- (19) Andrews, A. B.; McClelland, A.; Korkeila, O.; Demidov, A.; Krummel, A.; Mullins, O. C.; Chen, Z. Molecular Orientation of Asphaltenes and PAH Model Compounds in Langmuir–Blodgett Films using Sum Frequency Generation Spectroscopy. *Langmuir* **2011**, *27*, 6049-6058.
- (20) Ruiz-Morales, Y.; Mullins, O. C. Coarse-Grained Molecular Simulations to Investigate Asphaltenes at the Oil–Water Interface. *Energy Fuels* **2015**, *29*, 1597-1609.
- (21) Gao, F.; Xu, Z.; Liu, G.; Yuan, S. Molecular Dynamics Simulation: The Behavior of Asphaltene in Crude Oil and at the Oil/Water Interface. *Energy Fuels* **2014**, *28*, 7368-7376.
- (22) Teklebrhan, R. B.; Ge, L.; Bhattacharjee, S.; Xu, Z.; Sjöblom, J. Initial Partition and Aggregation of Uncharged Polyaromatic Molecules at the Oil-Water Interface: A Molecular Dynamics Simulation Study. *The Journal of Physical Chemistry B* **2014**, .
- (23) Kuznicki, T.; Masliyah, J. H.; Bhattacharjee, S. Aggregation and Partitioning of Model Asphaltenes at Toluene– Water Interfaces: Molecular Dynamics Simulations. *Energy Fuels* **2009**, *23*, 5027-5035.
- (24) Mikami, Y.; Liang, Y.; Matsuoka, T.; Boek, E. S. Molecular Dynamics Simulations of Asphaltenes at the oil–water Interface: From Nanoaggregation to Thin-Film Formation. *Energy Fuels* **2013**, *27*, 1838-1845.

- (25) Liu, J.; Zhao, Y.; Ren, S. Molecular Dynamics Simulation of Self-Aggregation of Asphaltenes at an Oil/Water Interface: Formation and Destruction of the Asphaltene Protective Film. *Energy Fuels* **2015**, *29*, 1233-1242.
- (26) Jian, C.; Tang, T.; Bhattacharjee, S. Probing the Effect of Side Chain Length on the Aggregation of a Model Asphaltene using Molecular Dynamics Simulations. *Energy Fuels* , .
- (27) Jian, C.; Tang, T.; Bhattacharjee, S. Molecular Dynamics Investigation on the Aggregation of Violanthrone78-Based Model Asphaltenes in Toluene. *Energy Fuels* **2014**, .
- (28) Jian, C.; Tang, T. One-Dimensional Self-Assembly of Poly-Aromatic Compounds Revealed by Molecular Dynamics Simulations. *The Journal of Physical Chemistry B* **2014**, .
- (29) Jian, C.; Tang, T. Molecular Dynamics Simulations Reveal Inhomogeneity-Enhanced Stacking of Violanthrone-78-Based Polyaromatic Compounds in n-Heptane–Toluene Mixtures. *The Journal of Physical Chemistry B* **2015**, *119*, 8660-8668.
- (30) Schuler, B.; Meyer, G.; Peña, D.; Mullins, O. C.; Gross, L. Unraveling the Molecular Structures of Asphaltenes by Atomic Force Microscopy. *J. Am. Chem. Soc.* **2015**, *137*, 9870-9876.
- (31) Sato, T.; Araki, S.; Morimoto, M.; Tanaka, R.; Yamamoto, H. Comparison of Hansen Solubility Parameter of Asphaltenes Extracted from Bitumen Produced in Different Geographical Regions. *Energy Fuels* **2014**, *28*, 891-897.
- (32) Yang, F.; Tchoukov, P.; Dettman, H.; Teklebrhan, R. B.; Liu, L.; Dabros, T.; Czarnecki, J.; Masliyeh, J.; Xu, Z. Asphaltene Subfractions Responsible for Stabilizing Water-in-Crude Oil Emulsions. Part 2: Molecular Representations and Molecular Dynamics Simulations. *Energy Fuels* **2015**, *29*, 4783-4794.
- (33) Shi, M.; Chen, Y.; Nan, Y.; Ling, J.; Zuo, L.; Qiu, W.; Wang, M.; Chen, H. P- p Interaction among Violanthrone Molecules: Observation, Enhancement, and Resulting Charge Transport Properties. *The Journal of Physical Chemistry B* **2010**, *115*, 618-623.
- (34) Shi, M.; Hao, F.; Zuo, L.; Chen, Y.; Nan, Y.; Chen, H. Effect of Substituents on the Aggregate Structure and Photovoltaic Property of Violanthrone Derivatives. *Dyes and Pigments* **2012**, *95*, 377-383.
- (35) Eley, D.; Hey, M.; Symonds, J. Emulsions of Water in Asphaltene-Containing Oils 1. Droplet Size Distribution and Emulsification Rates. *Colloids and surfaces* **1988**, *32*, 87-101.
- (36) Peng, L.; Liu, C.; Kwan, C.; Huang, K. Optimization of Water-in-Oil Nanoemulsions by Mixed Surfactants. *Colloids Surf. Physicochem. Eng. Aspects* **2010**, *370*, 136-142.

- (37) Berendsen, H. J. C.; Postma, J. P. M.; van Gunsteren, W.; Hermans, J. In *Interaction Models for Water in Relation to Protein Hydration*. Pullmann, B., Ed., Ed.; In Intermolecular Forces; D. Reidel Publishing Company: Dordrecht, 1981.; pp 331-342.
- (38) Tieleman, D.; Berendsen, H. Molecular Dynamics Simulations of a Fully Hydrated Dipalmitoylphosphatidylcholine Bilayer with Different Macroscopic Boundary Conditions and Parameters. *J. Chem. Phys.* **1996**, *105*, 4871-4880.
- (39) Zielkiewicz, J. Structural Properties of Water: Comparison of the SPC, SPCE, TIP4P, and TIP5P Models of Water. *J. Chem. Phys.* **2005**, *123*, 104501.
- (40) Schüttelkopf, A. W.; Van Aalten, D. M. F. PRODRG: A Tool for High-Throughput Crystallography of Protein-Ligand Complexes. *Acta Crystallographica Section D: Biological Crystallography* **2004**, *60*, 1355-1363.
- (41) Oostenbrink, C.; Villa, A.; Mark, A. E.; Van Gunsteren, W. F. A Biomolecular Force Field Based on the Free Enthalpy of Hydration and Solvation: The GROMOS Force-Field Parameter Sets 53A5 and 53A6. *Journal of Computational Chemistry* **2004**, *25*, 1656-1676.
- (42) Lemkul, J. A.; Allen, W. J.; Bevan, D. R. Practical Considerations for Building GROMOS-Compatible Small-Molecule Topologies. *Journal of Chemical Information and Modeling* **2010**, *50*, 2221-2235.
- (43) Pisula, W.; Tomovic, Z.; Simpson, C.; Kastler, M.; Pakula, T.; Müllen, K. Relationship between Core Size, Side Chain Length, and the Supramolecular Organization of Polycyclic Aromatic Hydrocarbons. *Chemistry of materials* **2005**, *17*, 4296-4303.
- (44) Hess, B.; Kutzner, C.; van der Spoel, D.; Lindahl, E. GROMACS 4: Algorithms for Highly Efficient, Load-Balanced, and Scalable Molecular Simulation. *Journal of chemical theory and computation* **2008**, *4*, 435-447.
- (45) Van Der Spoel, D.; Lindahl, E.; Hess, B.; Groenhof, G.; Mark, A. E.; Berendsen, H. J. GROMACS: Fast, Flexible, and Free. *Journal of computational chemistry* **2005**, *26*, 1701-1718.
- (46) Lindahl, E.; Hess, B.; Van Der Spoel, D. GROMACS 3.0: A Package for Molecular Simulation and Trajectory Analysis. *Journal of Molecular Modeling* **2001**, *7*, 306-317.
- (47) Berendsen, H. J.; van der Spoel, D.; van Drunen, R. GROMACS: A Message-Passing Parallel Molecular Dynamics Implementation. *Comput. Phys. Commun.* **1995**, *91*, 43-56.
- (48) Parrinello, M.; Rahman, A. Polymorphic Transitions in Single Crystals: A New Molecular Dynamics Method. *J. Appl. Phys.* **1981**, *52*, 7182-7190.
- (49) Bussi, G.; Donadio, D.; Parrinello, M. Canonical Sampling through Velocity-Rescaling. *arXiv preprint arXiv:0803.4060* **2008**, .

- (50) Miyamoto, S.; Kollman, P. A. **Settle: An Analytical Version of the SHAKE and RATTLE Algorithm for Rigid Water Models.** *J. Comput. Chem.* **1992**, *13*, 952-962.
- (51) Hess, B. P-LINCS: A Parallel Linear Constraint Solver for Molecular Simulation. *Journal of Chemical Theory and Computation* **2008**, *4*, 116-122.
- (52) Essmann, U.; Perera, L.; Berkowitz, M. L.; Darden, T.; Lee, H.; Pedersen, L. G. A Smooth Particle Mesh Ewald Method. *J. Chem. Phys.* **1995**, *103*, 8577.
- (53) Humphrey, W.; Dalke, A.; Schulten, K. VMD: Visual Molecular Dynamics. *J. Mol. Graph.* **1996**, *14*, 33-38.
- (54) David, S.; Hess, B. Gromacs User Manual. Version 4.0. *Netherlands: University of Groningen* **2006**, .
- (55) Speight, J. G.; Long, R. B.; Trowbridge, T. D. Factors Influencing the Separation of Asphaltenes from Heavy Petroleum Feedstocks. *Fuel* **1984**, *63*, 616-620.
- (56) Yarranton, H. W.; Alboudwarej, H.; Jakher, R. Investigation of Asphaltene Association with Vapor Pressure Osmometry and Interfacial Tension Measurements. *Industrial and Engineering Chemistry Research* **2000**, *39*, 2916-2924.
- (57) Acevedo, S.; Castro, A.; Vásquez, E.; Marcano, F.; Ranaudo, M. A. Investigation of Physical Chemistry Properties of Asphaltenes using Solubility Parameters of Asphaltenes and their Fractions A1 and A2. *Energy Fuels* **2010**, *24*, 5921-5933.
- (58) Jian, C.; Tang, T.; Bhattacharjee, S. A Dimension Map for Molecular Aggregates. *J. Mol. Graph. Model.* **2015**, *58*, 10-15.
- (59) Gao, S.; Moran, K.; Xu, Z.; Masliyah, J. Role of Naphthenic Acids in Stabilizing Water-in-Diluted Model Oil Emulsions. *The Journal of Physical Chemistry B* **2010**, *114*, 7710-7718.
- (60) Grimes, B.; Dorao, C.; Simon, S.; Nordgård, E.; Sjöblom, J. Analysis of Dynamic Surfactant Mass Transfer and its Relationship to the Transient Stabilization of Coalescing liquid-liquid Dispersions. *J. Colloid Interface Sci.* **2010**, *348*, 479-490.